

# Improving the chemical homogeneity of austenitic and martensitic stainless steels during nitrogen alloying in the pressure electro slag remelting (PESR) process

M. Bartosinski<sup>1</sup>, John H. Magee<sup>2</sup>, B. Friedrich<sup>1</sup>

<sup>1</sup>IME Process Metallurgy and Metal Recycling, RWTH Aachen University, Intzestr. 3, 52056 Germany

<sup>2</sup>Carpenter Technology, Corp, 101 W Bern St, Reading PA 19610, USA

Keywords: pressure electroslag remelting, high nitrogen steels

## Abstract

Due to their high strength and corrosion resistance, high nitrogen stainless steels are becoming an increasingly important group of materials. As austenite stabilizer, nitrogen can lead to the partial substitution of nickel. However, nitrogen-alloying of steels exhibits unique challenges since the nitrogen solubility in liquid iron at standard pressure is very low (~0.045 wt.-%).

Pressure Electro Slag Remelting (PESR) has emerged as the most robust process for producing high nitrogen steels. In this process nitrogen is introduced into the melt by dissolving nitrogen bearing additives during remelting. Besides achieving the desired nitrogen level, the major challenge with this process is its homogeneous distribution to ensure uniform material properties. In the present investigation, several remelting trials were conducted at a laboratory scale 400 kW-PESR furnace with the goal of attaining high nitrogen austenitic and martensitic steel ingots with a homogeneous N-content of 0.8 wt.-% and 0,35 wt.-%, respectively. Preliminary trials suggested the use of granulated  $\text{Si}_3\text{N}_4$  as the most effective nitrogen source. Small ingots of 160 mm diameter were cast, sectioned, etched, characterized and their composition was analysed.

Results show that the most important factors for adjusting a constant nitrogen activity in the slag and therefore a homogeneous distribution of nitrogen in the ingot are an accurate feeder calibration prior to the trials as well as constant melt and  $\text{Si}_3\text{N}_4$ -feeding rates during remelting. Furthermore, both the feeder accuracy and the nitrogen yield were calculated. The results show a nitrogen recovery of 40-54 %. An equation was set up in order to determine the required  $\text{Si}_3\text{N}_4$  amount during the remelting process, accounting for the calculated yield factors.

## Introduction

More than 60 years ago first attempts were made to replace nickel as an expensive and scarce alloying element with nitrogen because of its strong stabilizing effect on the austenitic structure without loss of strength or corrosion resistance. [1] In the 21st century, scarcity of nickel is not the critical issue, but rather the volatility in its price. In 2006-07, the London Metal Exchange (LME) price of nickel went from \$ 6 to \$ 23 per pound. This has led metallurgists to consider alternative low nickel, high nitrogen alloys, especially when their current stainless alloy contains 12-30 % Ni. Beside of the economic aspect, nitrogen offers metallurgical property advances in many respects as an alloying element for stainless steels. [2]

For example, with the elimination of nickel the alloy is more suitable for biomedical applications where nickel-free alloys are sought out when allergic reactions are a concern. Beside of this, stainless steel alloys have superior pitting corrosion properties when nitrogen is used as a substitute for carbon. Nitrogen is a more effective solid-solution strengthener than carbon and has a greater solid-solubility, decreasing the tendency for precipitation at a given level of strengthening. [3][5] Also, high nitrogen martensitic stainless steels show improved resistance to localized corrosion (pitting, crevice and intergranular corrosion) over their carbon containing counterparts. [4]

In conventional steel making, nitrogen is often introduced into the melt using either a master alloy, like ferro-chrome nitride, or in a process like Argon Oxygen Decarburization (AOD), where it can be blown into the melt. However, in these processes, the maximum amount of nitrogen that can be added to the alloy is limited by its solubility at the casting temperature under atmospheric pressure. Although the solubility under these conditions is very low, nitrogen levels above 1 wt.-% can be obtained through different alloying elements and high-pressure melting techniques. Steel should be considered high nitrogen, if it contains more nitrogen than the solubility limit at atmospheric pressure. [5]

Today, the pressurized electroslag remelting process is commonly used for steel grades with nitrogen levels exceeding the 1 bar solubility limit. Since common ESR slags have virtually no solubility for nitrogen, the element is introduced to the melt in form of nitrogen bearing additives, such as FeCrN or Si<sub>3</sub>N<sub>4</sub>, during remelting. The nitrogen pressure above the melt serves to keep the desired nitrogen level in the molten metal. [2] Main challenge during electroslag remelting is not only increasing the nitrogen level, but also its homogeneous distribution in the product.

This paper presents a part of a research program between Carpenter R&D and IME Process Metallurgy and Metal Recycling Aachen. Main object of this study was the PESR of Carpenter's 15-15HS and X30CrMoN151 alloy with the focus of rising the nitrogen level homogeneously above the solubility limit with the expectation of enhanced mechanical and corrosion properties. The material used for this lab scale trials was produced at Carpenter R&D's Vacuum Induction Furnace (VIM) and then remelted in a PESR furnace in Aachen.

## Fundamentals

### Nitrogen solubility

Nitrogen solubility and production of high nitrogen steels was part of many publications (i.e [6] and [7]). Here, the most important fundamentals for the understanding of this study are presented.

For a diatomic gas like nitrogen, the solubility reaction in liquid iron can be generally written as [6]:



The standard free energy of equation (1) can be used to calculate the equilibrium constant,  $K_{eq}$ , which can be used to relate the solubility (given in weight percent) to partial pressure [6]:

$$K_{eq} = \frac{f_N^{[%N]}}{p_{N_2}^{0.5}} \quad (2)$$

where  $p_{N_2}$  is the partial pressure of nitrogen in bar and  $f_N$  is the nitrogen activity coefficient. The following equation is used to calculate the activity coefficient for nitrogen, which includes 2<sup>nd</sup> order terms to account for high alloying element levels [2]:

$$\log f_N = \sum e_N^j [%j] + \sum r_N^j [%j]^2 + \sum r_N^{j-k} [%j][%k] \quad (3)$$

As mentioned before, the low solubility of nitrogen in liquid iron at atmospheric pressure is the major challenge during production of high nitrogen steels. Generally, the saturation solubility closely follows Sievert's Law and is proportional to the square root of the N<sub>2</sub> gas pressure above the melt. In stainless and

related alloys, deviations from the law can occur at elevated pressures high above one atmosphere. To account for the deviation a self-interaction parameter must be included for the calculation of the nitrogen activity coefficient, caused by the dense packaging of nitrogen atoms in the melt structure [7].

Figure 1 shows the temperature dependency of nitrogen solubility in Fe and Fe-Cr binary alloys at 1 bar pressure, which is an important topic for the melting practice of high nitrogen steels. A negative temperature dependency is noticeable with a rapid decrease in the ferritic structure. If there is ferritic solidification, a noticeable decrease of nitrogen solubility occurs, which may lead to the formation of pores and/or nitrides. With increasing Cr content there is a huge increase in the solubility. While gas solubilities in metals generally decrease with decreasing temperature, this is just the opposite in Fe-Cr alloy. This effect occurs with all solubility increasing elements. Figures 2 and 3 show that the nitrogen solubility in iron is, beside temperature, controlled by nitrogen gas pressure and the addition of alloying elements. Additions of chromium, manganese and molybdenum increase the solubility of N and are the best choice for production of alloys with a combination of superior strength, toughness and corrosion resistance. Although elements such as titanium and vanadium can have a greater effect on solubility, they readily form stable nitrides, which will already precipitate at very low nitrogen concentrations. Nickel, silicon and carbon decrease N solubility.

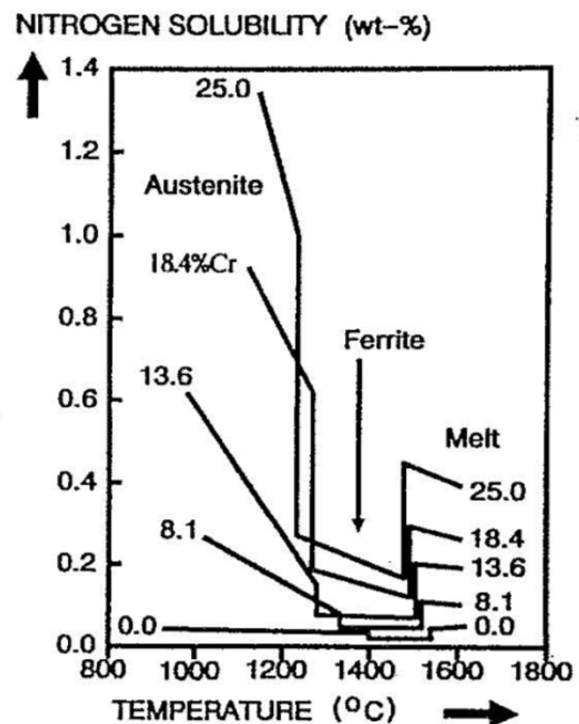


**Figure 1:** Influence of Temperature on the nitrogen solubility of binary Fe-Cr-alloys at 1 bar pressure, after [6]

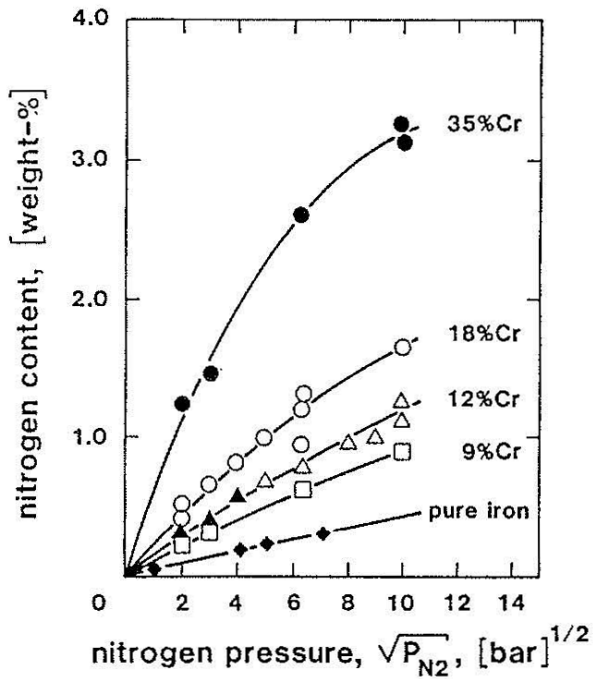


**Figure 2:** Influence of nitrogen gas pressure and chromium on the nitrogen content in iron at 1600°C, after [6]

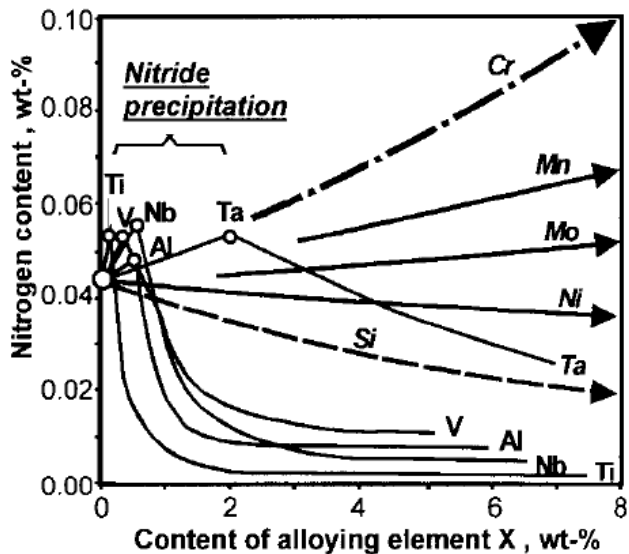


**Figure 3:** Influence of different alloying elements on nitrogen content in a binary Fe-X alloy at 1600°C and 1 bar pressure, after [6]

Electroslag Remelting (ESR)

The electroslag remelting is a metallurgical refining process to obtain ingots with higher purity concerning inclusions and a homogeneous microstructure. Though first experiments dealing with the remelting of metal through slag were made in the 1930's, the development of industrial ESR plants took place in the 1950's ([9],[10]). Today, the process is widely used in the steel industry and for the production of

superalloys.

Characteristic for this process is the use of a water cooled copper crucible to avoid any reactions between the liquid metal and the crucible walls. The material to be refined is used as a self-consuming electrode, which is dipped into a molten slag bath. The impressed voltage between the electrode and the crucible bottom plate drops in the slag bath, which operates as a resistance heating. As a consequence, droplets detach from the electrode tip and sink through the slag and are collected in a liquid metal pool. Refining reactions, such as dissolution or flotation of nonmetallic inclusions, take place between the liquid slag and metal.

Depending on the furnace complexity, the gas atmosphere composition, furnace pressure and the slag chemistry can be adjusted (figure 4). Using the ESR process for nitrogen alloying of steel, the slag represents a strong barrier to nitrogen transfer from the gas atmosphere to the metal pool. This obstacle can be overcome by the addition of a suitable nitride to the slag during remelting, for example  $Si_3N_4$ . As a consequence, nitrogen solubilities of several percent can be reached within short times due to the fact, that upon dissolution of the silicon nitride,  $N^{3-}$ -ions readily are formed avoiding the energetically unfavorable step of breaking up the stable  $N_2$  gas molecule. [7],[8]

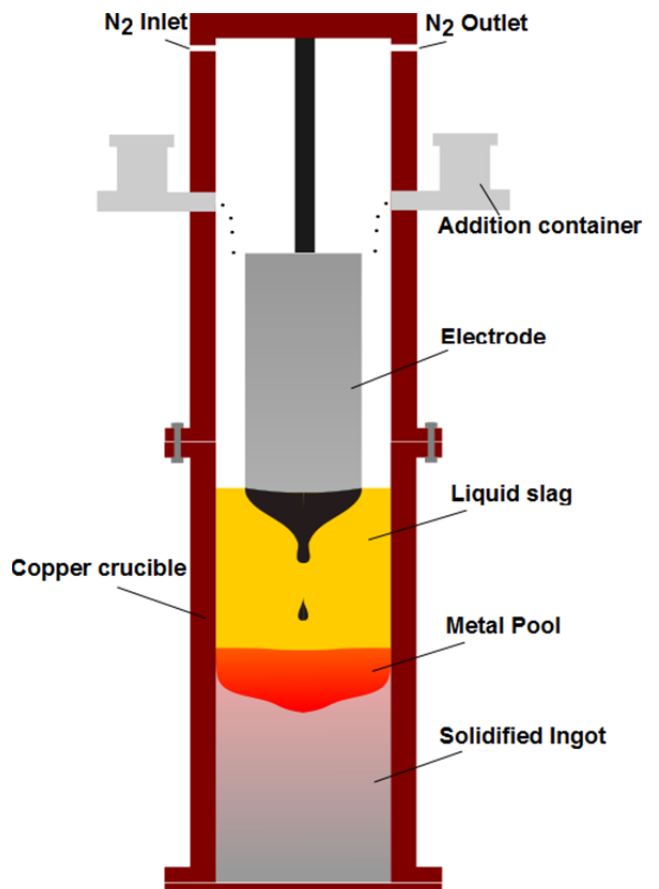


**Figure 4:** Schematic figure of the PESR process for nitrogen alloying

## Experimental Work

The conducted trials presented in this paper were part of a research program dealing with the PESR nitrogen alloying of steels. In the first part of this program the effects of furnace pressure and different nitrogen bearing additives on the solubility in a high chrome, high manganese austenitic steel (15-15HS® and BioDur®108 Alloy) were examined. The results were presented by Reitz and Patel [2].

The focus of the presented trials besides rising the nitrogen content above the solubility limit was especially achieving a uniform distribution in the ingots. Furthermore, two martensitic alloy electrodes were pressure remelted to obtain higher N-values as well. The electrodes for the trials were cast using a laboratory scale Vacuum Induction Melting (VIM) furnace with an equilibrium nitrogen content from 0.1–0.61 wt.-% depending on the alloy (table 1). A summary of the trial parameters are shown in table 2. The results from the first phase of the project lead to the use of Si<sub>3</sub>N<sub>4</sub> in granulated form instead of powder as nitrogen bearing additive. Furthermore, a process pressure of at least 5 bar was adjusted. The feed rate set point (FR) of the additive was determined by using the following relationship:

$$FR = \frac{\Delta N}{N_{Si_3N_4} \eta_{Si_3N_4} \eta_{feeder}} \dot{m} \quad (4)$$

Where  $\Delta N$  is the difference between the nitrogen content of the ingot and electrode,  $N_{Si_3N_4}$  is the percentage of nitrogen in the additive (here: 40 %),  $\dot{m}$  is the melt rate set point and  $\eta_{Si_3N_4}/\eta_{feeder}$  are yield factors for the additive and feeder to account for possible nitrogen losses. The latter two were adjusted after each trial. The melt rate set point was 1.6 kg/min.

**Table 1:** Electrode compositions

alloy	Cr	Mn	Ni	Mo	C
15-15HS® (austenitic)	19	18	0.3	1	0.03
X30CrMoN151 (martensitic)	15	0.5		1	0.30

**Table 2:** Trial parameters

melt no.	alloy	$m_{\text{Electrode}}$ /kg	$N_{\text{Electrode}}$ /wt%	$N_{\text{target}}$ /wt.-%	p /bar	feed rate /g/min
1	15-15	76.2	0.61	0.81	5	10.06
2	15-15	76.2	0.61	0.81	10	20.12
3	alloy 30	66.6	0.10	0.35	8	16.35
4	alloy 30	63.6	0.19	0.35	10	16.35

The PESR furnace located at IME, RWTH Aachen University used for the trials (figure 5) is capable of operating under inert-gas at a maximum pressure of 50 bar. It is equipped with a 5 kA power supply and a new control and monitoring system. The nominal electrode diameter is 110 mm, and the ingot diameter is 160 mm, slightly conical. The furnace is equipped with two bunkers and screw feeders for introducing additives during remelting. The feeders are driven by pneumatic cylinders which turn the feeder screw by a wrench-like set-up in 90° steps. With every turn, a controlled amount of the additive is extracted from the respective bunker and charged to the melt. The number of wrenching impulses per minute can be set independently for every feeder in the furnace control system. The furnace interior, the bunkers, and the cooling water are all maintained at the operating pressure. This furnace is not equipped with load cells, and the melt rate is precisely calculated from ram travel. For a smooth start-up, turnings are used with slag in the annular region between the electrode and crucible.



**Figure 5:** ESR/PESR furnaces at IME Aachen

As mentioned before, the silicon nitride was in granulated form of about 1-2 mm size. The feed rate of the bunkers was calibrated before the trials at different feeding speeds and furnace pressures. Calibration yields a linear relationship between impulses/minute of the pneumatic cylinders and g/min of charged additive. The pressure trials revealed a slight decrease of the feeding rate with increasing furnace pressure.



For start-up, nearly one kilogram of low carbon construction steel turnings was used. The turnings were placed in a bin located on the starter plate of the crucible. The crucible was then positioned over the starter plate, and the entire assembly was secured. The crucible was lowered into the furnace tank, and the electrode that was attached to the ram was lowered into the crucible. Then, 4 kg of a  $\text{CaF}_2$  32.5 %/  $\text{CaO}$  29.5 %/  $\text{MgO}$  2.2 %  $\text{Al}_2\text{O}_3$  30 %  $\text{SiO}_2$  1.1 % slag (Wacker 2015) was distributed around the turnings, in the annular region between the electrode and crucible. After this, the additives were charged into the feeding bunkers with the total weight split between the two. Both feeders were sealed and primed for 60 seconds which has proven to be sufficient to assure adequate feeding. The furnace head was then bolted on, cooling water circuits were started, and the melting chamber was evacuated down to 1 mbar with a vacuum pump and backfilled with nitrogen up to the desired pressure. The furnace was then ready for melting.

The process was started in electric arc mode under current control with a set-point of 4 kA at 28 V. After the slag was completely molten, current control was superseded by a constant power control at 110 kW with a quick ramp-up to 130 kW and slow ramp-down to 105 kW after the start-up. With the switch to power control, electrode immersion/ram travel was subjected to resistance control at a set-point of 12 mOhm. After the 130 kW power-up, ram-travel was refined by swing control at a set-point of 10 % of the absolute slag resistance. Simultaneously with the switch to power control, feeding of the nitrogen additive was ramped up to the desired feed rate. At the end of the melt, a short hot-topping phase was initiated.

Typical variations of voltage, current, melt rate and furnace pressure during the melt are shown in Figures 6 and 7 for an austenitic and martensitic alloy. A short duration after the melt was completed, the furnace pressure was released and the furnace seal was broken. The furnace was unbolted, and the ingot was extracted from the crucible and weighed (figure 8). The slag cap was measured, weighed, manually broken and sealed in plastic bags to avoid moisture pickup. The feeders were emptied and leftover  $\text{Si}_3\text{N}_4$  weighed for mass balance. On the rim of the crucible, amounts of flue-dust and uncharged nitride were noted.

The martensitic ingots were heat treated for 4 h at 670 °C after remelting and air cooled.

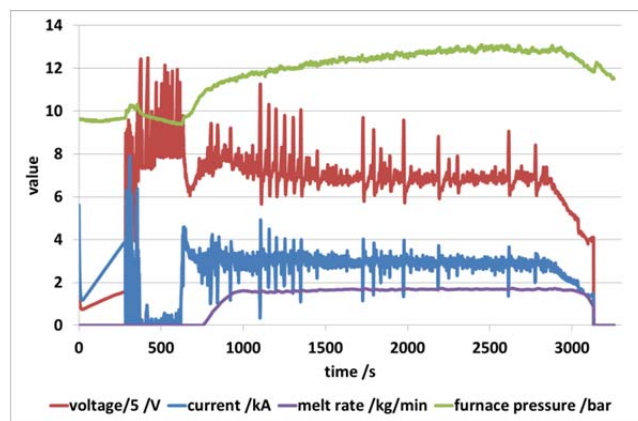


**Figure 6:** Voltage, current, melt rate and furnace pressure variation during remelting (15-15HS)

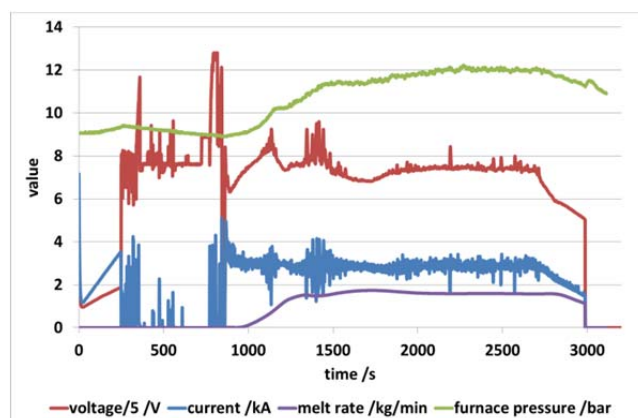


**Figure 7:** Voltage, current, melt rate and furnace pressure variation during remelting (X30CrMoN151)



**Figure 8:** Obtained ingot after PESR nitriding

## Results and Discussion

For a representative ingot characterization, a plate of the center longitudinal section was cut out and etched. The etching step was necessary to reveal possible defects such as porosity or macrosegregation. The plate surfaces after etching for both 15-15HS and X30CrMoN151 alloy are shown in figure 9. The structure is sound and typical for ESR ingots, with columnar grains from surface to ingot center at 45 degrees to the vertical axis. The macro structure from the other two ingots was identical to that shown in figure 9.

Next, these plates were cut into small 3 x 3 cm pieces. The nitrogen and silicon content of each piece was measured by Optical Emission Spectrometry (OES). The results for all four ingots are shown in the form of contour plots in figures 10 thru 13 with the ingot diameter on the horizontal axis, and ingot height on the vertical axis. Note that an ingot height of "0" is the top of ingot.



**Figure 9:** Ingot macrostructure after etching, left: 15-15HS, right: X30CrMoN151

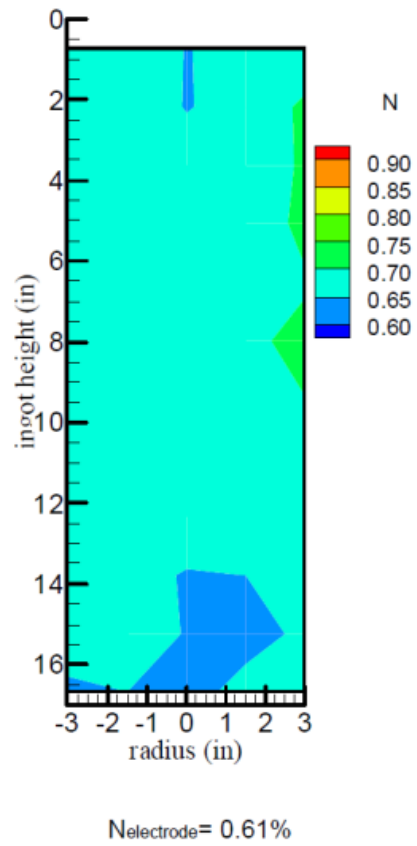


**Figure 10:** measured N content in ingot 1

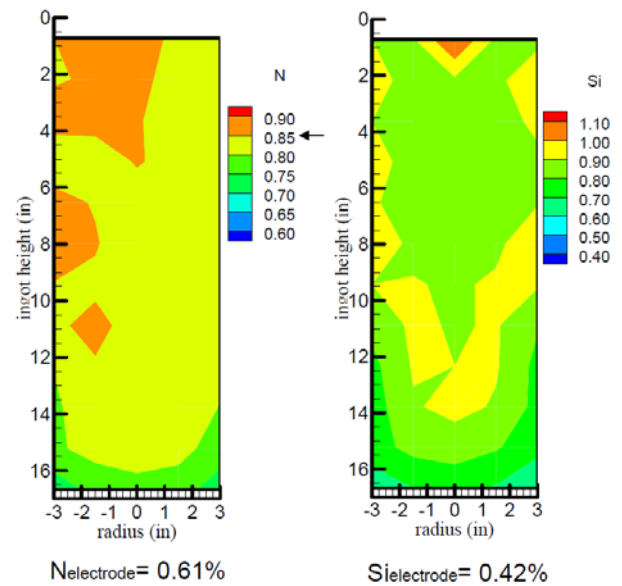


**Figure 11:** measured N and Si content in ingot 2

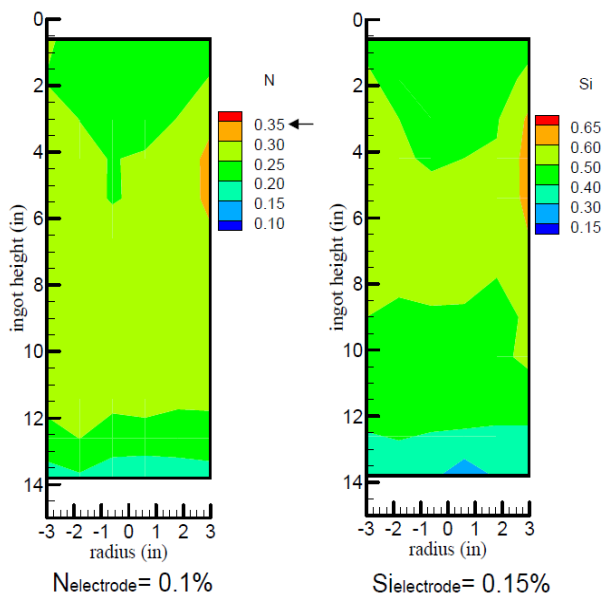


Figure 11: measured N and Si content in ingot 3

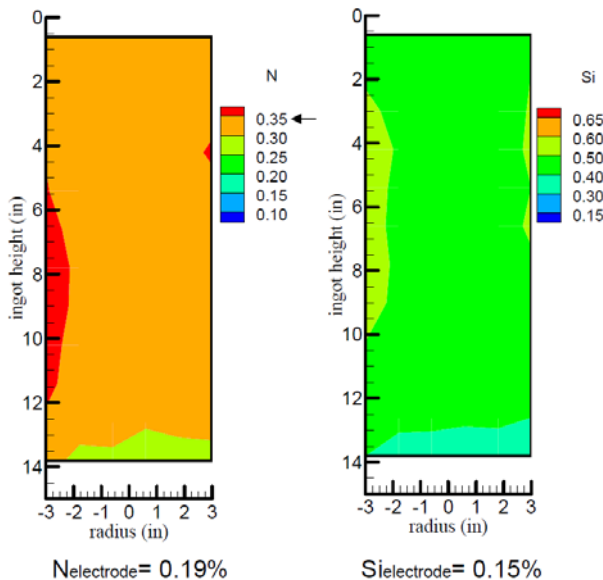


Figure 11: measured N and Si content in ingot 4

As the above figures show, an increase of nitrogen in all trials has been achieved. After missing the target nitrogen content of 0.85 % in the first trial, both the furnace pressure and the  $\text{Si}_3\text{N}_4$  feed rate were raised to account for the apparent nitrogen loss. However it should be noted, that the nitrogen distribution was homogeneous. These measures resulted in shifting the nitrogen content to the desired level (figure 10) although a decrease at the bottom is noticeable in all ingots. This is typical for ESR trials due to the fact that a starter bin filled with low alloyed steel was used.

The same observations can be made by evaluating the martensitic alloy trials 3 and 4. While the nitrogen level rises continuously from bottom to middle (0.26 %), it decays to the very top of the ingot (0.21 %). The target level of 0.35 % was missed.

After raising the necessary feed rate in trial 4, a very homogeneous distribution of nitrogen at the desired level was reached. When analysing the radial distribution of nitrogen, an asymmetry in form of slightly higher values at the edge can be noticed. This can be explained due to the fact that only one feeder for charging the additive was used and the slag flow was too weak to compensate the inhomogeneous distribution of silicon nitride.

Note that especially in trials 3 and 4 silicon follows nitrogen distribution qualitatively. In theory a 1.5 higher increase of silicon than nitrogen is expected when calculating, according to the S/N ratio of the nitride. But when looking at the results, a higher silicon increase can be noted. A summary of the achieved average N and Si contents shows table 3

Table 3: Average N and Si contents

ingot	$N_{\text{average}}/\text{wt.}\%$	$Si_{\text{average}}/\text{wt.}\%$
1	0.67	-
2	0.84	0.89
3	0.26	0.5
4	0.33	0.47

Trial 1 was conducted as a pilot test assuming that nitrogen recovery was 100 % and no further losses will occur. The measured N in the ingot was therefore lower than expected.

Due to the pressure rise according to figures 6 and 7 it can be assumed that there is some nitrogen loss to the atmosphere during remelting. Another explanation for the low N content is, that nitrogen stays undissolved as  $\text{Si}_3\text{N}_4$  in the slag. Slag analysis show N contents between 0.6 % and 1.4 %, but it is hard to quantify to what extent the silicon nitride and the  $\text{N}_2$  atmosphere above the melt are the source for the nitrogen pickup. Further lab scale trials with the focus on slag chemistry and dissolution of nitrogen in molten slags are needed to quantify these losses. Furthermore, the average  $\Delta\text{Si}/\Delta\text{N}$  ratio in the trials was around 2.3 (expected: 1.5), which confirms nitrogen losses. Furnace-specific factors like feeder accuracy also play an important role to ensure ingot homogeneity, due to the fact that uncharged nitride was noted at the crucible rim.

The recovery for nitrogen calculated from the average value is approx. 42 % for the martensitic and 50 % for the austenitic melts. The average silicon recovery is 66 % and 77 %. The reason for the lower recovery in the martensitic alloys has yet to be determined.

In general, the ingot homogeneity in these trials was improved in comparison to the first phase of this project as shown in Figure 12. It presents nitrogen and silicon contents in a 15-15 steel ingot after PESR nitriding. In this trial,  $\text{Si}_3\text{N}_4$  powder mixed with sand



was used to ensure proper feeding. The process pressure was set to 4 bar. Goal was a nitrogen rise from 0.4 % in the electrode to 0.6 %. A gradual and continuous decrease of both silicon and nitrogen with ingot height can be noticed, which is largely attributed to inadequate feeding during the melt and nitrogen/silicon recovery. Furthermore, the melt rate during the steady addition of silicon nitride was not nearly uniform, and hence there was a discrepancy between the feed rate set point and desired feed rate. As figures 6 and 7 show, the melt rate uniformity was greatly improved in the trials presented in this paper.

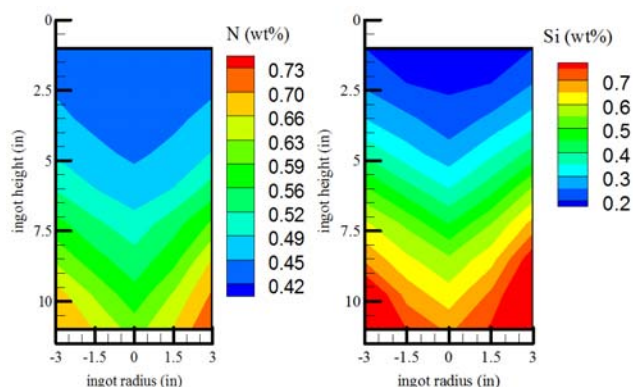


**Figure 12:** 15-15HS® alloy after PESR (phase 1)

## Conclusion

Experiments were conducted on a laboratory scale PESR furnace in order to raise the nitrogen level homogeneously above the solubility limit. Four electrodes made of two different steel alloys were remelted at pressures from 5 to 10 bar.  $\text{Si}_3\text{N}_4$  granules were used as nitrogen bearing additive. Results show, that the nitrogen level was higher than in the electrodes and that nitrogen uniformity was significantly improved as a result of altering the  $\text{Si}_3\text{N}_4$  feed rate and rising the process pressure to 10 bar. Constant feeding and constant melt rates are two important factors for the production of sound ingots. The use of silicon nitride in granulated form improved nitrogen homogeneity significantly

As a consequence for the huge variations between the theoretical feed rate and the feed rate actually used in the trials to achieve the desired nitrogen level, a yield factor for nitrogen has to be introduced in order to compensate nitrogen losses during the trial by adjusting the feed rate to higher values. According to the results the reached nitrogen yield is between 40 and 54 % depending on the alloy and furnace pressure. 54 % were reached in trial 2 while remelting the austenitic alloy at 10 bar. Nitrogen losses during the remelting have yet to be investigated.

## References

- [1] J.S. Dunning, J.W. Simmons, J.C. Rawers: Advanced Processing Technology for High-Nitrogen Steels, *Journal of Metals*, 1994, pp. 40-42
- [2] A.D. Patel, J. Reitz, J.H. Magee, R. Smith, G. Maurer, B. Friedrich: On Nitrogen Pick-Up During Pressure-ESR of Austenitic Steels, *International Symposium on Liquid Metal Processing and Casting*, TMS, 2009
- [3] A. Mitchell, F. Frederiksson: The electroslag remelting of high-nitrogen steels, *Proc. of 2003 Intl. Symp. on Liquid Metals*, *Journal of Materials Science*, Vol. 39, 2004, pp. 7275-7283
- [4] H. Leda: Nitrogen in martensitic stainless steels, *Journal of Materials Processing Technology*, Vol. 53, 1995, pp. 263-272
- [5] J.W. Simmons: Overview: high-nitrogen alloying of stainless steels, *Materials Science and Engineering A207*, 1996, pp. 159-169
- [6] A. Satir-Kolorz, H.K. Feichtinger, M.O. Speidel: On the Solubility of Nitrogen in Iron and Cast Steel Alloys at Elevated Pressure, *Giessereiforschung* 41, no. 4, 1989, pp. 149-165.
- [7] H. K. Feichtinger, G. Stein: Melting of High Nitrogen Steels, *Materials Science Forum*, Vols. 318-320, 1999, pp. 261-270.
- [8] H. Ono, K. Morita, N. Sano: Kinetic Studies on the Dissolution of Nitrogen in  $\text{CaO-Al}_2\text{O}_3$ ,  $\text{CaO-SiO}_2$  and  $\text{CaO-CaF}_2$  Melts, *Metallurgical and Materials Transactions B*, Vol. 28B, 1997, pp. 633-638
- [9] W.E. Duckworth, G. Hoyle: *Electro-Slag Refining*, British Iron and Steel, 1969, SBN 412 09670 6
- [10] G. Hoyle: *Electroslag Processes: Principles and Practice*, Applied Science Publishers, 1983, ISBN: 0-85334-164-8